PHYSICS

Two-photon induced coherence without induced emission

Dong-Gil Im*†, Seung-Yeun Yoo, Chung-Hyun Lee, Jongheon Suh, Yoon-Ho Kim*

At the heart of recent advances in quantum imaging and spectroscopy with undetected photons is the quantum optical effect known as induced coherence without induced emission. This quantum interference effect has enabled access to challenging wavelength regimes for imaging and spectroscopic applications. However, the potential of undetected photon quantum metrology, particularly the enhanced phase sensitivity offered by Fock or N00N states, has not yet been realized, as prior work focused only on single-photon phenomena. Here, we report the observation of two-photon induced coherence without induced emission. Using a two-photon Fock state, we establish quantum coherence between pairs of two-photon spontaneous emission amplitudes, resulting in a doubling of interferometric phase modulation. Specifically, we show that a phase shift ϕ applied to undetected 1016-nanometer photons leads to a 2ϕ modulation in the detection of 632-nanometer photons. This demonstrates genuine two-photon induced coherence without induced emission and opens possibilities for quantum-enhanced phase measurements using multiphoton coherence without detecting the modulated photons.

INTRODUCTION

Optical coherence, induced through light injection, plays a crucial role in numerous applications across photonics, spectroscopy, metrology, and communications. Such induced optical coherence arises from induced emission triggered by the injection of light (*1*–*3*). Unexpectedly, induced coherence without induced emission is possible in quantum optics (*4*, *5*), and it arises from the inherent indistinguishability of the probability amplitudes involved in the process (*6*–*9*). The phenomenon of induced coherence without induced emission is perhaps one of the most fascinating fundamental quantum optical interference effects, as it is uniquely observed in the first order in intensity (*8*, *10*–*12*), unlike most other quantum optical interference effects, which are exhibited in the second-order intensity-intensity correlation measurement (*13*–*15*). In addition to the fundamental importance and interest, this phenomenon forms a basis of nonlinear interferometry in quantum optics (*16*–*19*).

Recently, the phenomenon of induced coherence without induced emission has been leveraged to make substantial breakthroughs in quantum optical metrology using undetected photons, opening up possibilities in accessing challenging wavelength regimes, e.g., mid-infrared wavelengths, for quantum imaging (*20*–*25*), correlation imaging (*26*–*29*), quantum spectroscopy (*30*–*33*), quantum optical coherence tomography (*34*, *35*), and quantum polarimetry (*36*). In spite of these advancements, quantum-enhanced phase sensitivity, the hallmark effect in quantum metrology, has not been demonstrated for quantum metrology with undetected photons. This is because the exploration of induced coherence without induced emission has been limited to phenomena involving single photons.

In this study, we propose and experimentally demonstrate two-photon induced coherence without induced emission. This is achieved by using a two-photon Fock state in a nonlinear interferometer to induce quantum coherence among pairs of two-photon spontaneous emission amplitudes. The outcome is a doubling of the interferometric phase modulation compared to the modulation observed with single photons in quantum interferometry with undetected photons. Specifically, we demonstrate that applying a phase change ϕ to undetected 1016-nm near-infrared photons results in a 2ϕ modulation when detecting the 632-nm visible photons in our nonlinear interferometer, confirming the presence of two-photon induced coherence without induced emission.

RESULTS

Conceptual scheme

Consider the conceptual schematic of the nonlinear interferometer implementing induced coherence without induced emission in Fig. 1. The scheme for the ordinary induced coherence without induced emission is shown in Fig. 1A (*4*, *5*). Two identical second-order nonlinear crystals NL1 and NL2 are pumped simultaneously by the same ultraviolet pump laser, causing the generation of a pair of signal and idler photons, $S_1 - I_1$ from NL1 or $S_2 - I_2$ from NL2, via spontaneous parametric down-conversion (SPDC). Because the photon pair of SPDC is in a pure state, the signal (S_1 or S_2) and the idler photons (I_1 or I_2) individually are in thermal states (*37*, *38*), and therefore, no first-order interference is expected to occur by overlapping the two signal or the two idler modes. However, when the idler modes I_1 from NL1 is overlapped spatiotemporally with I_2 through NL2 as shown in Fig. 1A, nonclassical first-order interference occurs for the signal photon at detector D_1 or D_2 (*8*, *12*). Unexpectedly, the phase modulation ϕ_I introduced to the undetected idler photon is exhibited in the interference of the signal photon. If we choose the wavelength of the undetected idler photon in the near-infrared regime where photon detection is challenging, this nonlinear interferometer allows us to use the visible signal photon to measure the phase modulation ϕ_I. It is important to note that, while this scheme opens possibilities in accessing challenging wavelength regimes for quantum metrology, quantum-enhanced phase sensitivity cannot be achieved because this is still a single-photon effect.

Consider now the possibility of multiphoton induced coherence without induced emission, in which N signal-idler photon pairs could be generated either at NL1 or at NL2. The quantum state, in this

Department of Physics, Pohang University of Science and Technology (POSTECH), Pohang 37673, Korea.
*Corresponding author. Email: eastgil7902@gmail.com (D.-G.I.); yoonho72@gmail.com (Y.-H.K.)
†Present address: Agency for Defense Development, Daejeon 34186, Korea.

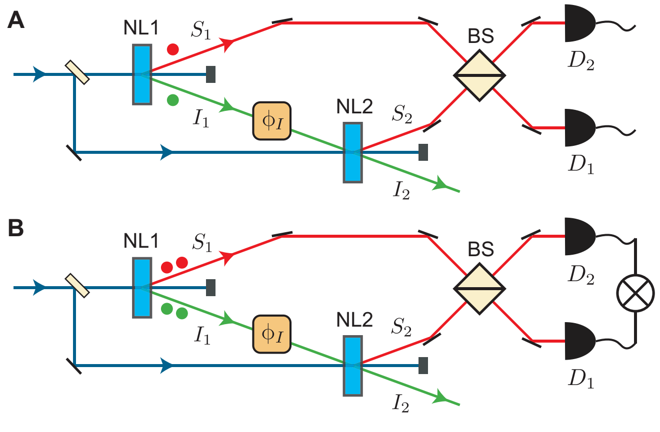

Fig. 1. Schematic of induced coherence without induced emission. (**A**) Ordinary induced coherence without induced emission is observed at detector D_1 or D_2 as single-photon interference. (**B**) Proposed two-photon induced coherence without induced emission. The effect is observed in coincidence between detectors D_1 and D_2.

case, can be written as $|\Psi_N\rangle = \frac{1}{\sqrt{2}}\left(e^{iN\phi_I}|N\rangle_{S_1}|N\rangle_{I_1} + |N\rangle_{S_2}|N\rangle_{I_2}\right)$, where the subscripts refer to the signal and idler modes as labeled in Fig. 1B. When N idler photons are injected into NL2 without induced emission, the idler modes become identical and quantum coherence is induced between the probability amplitudes for the signal photon $|N\rangle_{S_1}$ and $|N\rangle_{S_2}$. Thus, the phase change ϕ_I is applied to the undetected idler photon as in Fig. 1B, and the signal photon should exhibit $N\phi_I$ phase modulation or quantum-enhanced phase sensitivity (*39–44*), which is the hallmark effect in quantum metrology. Note that the significance of the induced coherence approach to quantum metrology is partly rooted in the fact that the signal photon could be in the visible regime where the detection is simple and efficient, while the idler photon could be in challenging wavelength regimes, such as near-infrared to mid-infrared.

Experimental results

We now describe the experimental demonstration of two-photon induced coherence without induced emission based on SPDC (see Fig. 1B). The quantum state of two pairs of photons, in this case, can be written as

$$|\Psi\rangle = \left(\frac{1}{2}e^{i2\phi_I}\hat{a}^{\dagger 2}_{S_1}\hat{a}^{\dagger 2}_{I_1} + \frac{1}{2}\hat{a}^{\dagger 2}_{S_2}\hat{a}^{\dagger 2}_{I_2} + e^{i\phi_I}\hat{a}^{\dagger}_{S_1}\hat{a}^{\dagger}_{S_2}\hat{a}^{\dagger}_{I_1}\hat{a}^{\dagger}_{I_2}\right)|0\rangle \quad (1)$$

where the normalization constant is omitted. For SPDC, when considering the probability amplitudes for two pairs of photons from two sources (NL1 and NL2), it is necessary to consider the probability amplitude for each source contributing a single photon pair, and this is represented in the third term in Eq. 1. This term does not carry the desired phase factor of $2\phi_I$, and we can exclude this term from contaminating our desired $2\phi_I$ modulation in the signal photon via the coincidence measurement between detectors D_1 and D_2 located at the output modes of BS, as shown in Fig. 1B. The identical single photons in modes S_1 and S_2 are overlapped at BS, and due to the Shih-Alley/Hong-Ou-Mandel interference (*13*), the third term in Eq. 1 only leads to the two-photon coalescence event either at D_1 or D_2, but never at the coincidence measurement. Thus, assuming perfect matching of the undetected photon modes I_1 and I_2, the joint detection probability P between D_1 and D_2 reveals the two-photon induced coherence without induced emission, exhibiting the quantum-enhanced phase sensitivity of $2\phi_I$

$$\mathcal{P} = 2 + 2\cos(2\phi_I) \quad (2)$$

The experimental setup is schematically shown in Fig. 2. An ultrafast femtosecond laser (Coherent Chameleon) with a central wavelength of 780 nm, a pulse duration of 140 fs [corresponding to a full width at half maximum (FWHM) bandwidth of ~6 nm], and a repetition rate of 80 MHz is first frequency doubled to 390 nm (FWHM bandwidth of 1.84 nm) using a 1.1-mm-thick lithium triborate (LBO) crystal. The resulting pulses are then used to pump a 1-mm-thick collinear type II beta-barium borate (BBO) crystal for signal-idler photon pair generation via SPDC. The signal photon wavelength is 632.8 nm, and the undetected idler photon wavelength is 1016.4 nm. We use a double-pass setup in which the residual forward pump pulse is retro-reflected back to the BBO crystal. The forward and backward SPDC processes in Fig. 2 correspond to NL1 and NL2 in Fig. 1B. The idler mode I_1 from the forward SPDC, corresponding to NL1 in Fig. 1B, is retro-reflected to the BBO to overlap with the I_2 mode of the backward SPDC, corresponding to NL2 in Fig. 1B, with the idler mirror. The idler mirror is controlled with a piezo actuator to add phase ϕ_I to the undetected idler photons. The signal modes S_1 and S_2 from the forward and backward SPDC, respectively, are overlapped at BS and two detectors D_1 and D_2 are positioned at the two outputs of BS. Because we make use of type II SPDC for the photon pair generation, the signal and idler photons of SPDC have tight frequency anticorrelation (*45*). This results in a mixed state for the quantum state of the signal photon, reducing the visibility of the Shih-Alley/Hong-Ou-Mandel interference in multiphoton quantum interference experiment (*46–48*). To remove the frequency anticorrelation, the 632.8-nm signal photons are passed through interference filters having a bandwidth of 2 nm at FWHM before detection. See the Supplementary Materials for details of the joint spectral intensity. Last, the single-detection and the joint-detection events from the two detectors are recorded as a function of the idler mirror position.

The main experimental results are shown in Fig. 3. As the idler mirror is translated using a piezo actuator, adding the phase factor ϕ_I to the undetected 1016.4 nm idler photons, detectors D_1 and D_2 registering the 632.8-nm signal photons exhibit the first-order single-photon quantum interference [see Fig. 3 (A and B)]. These

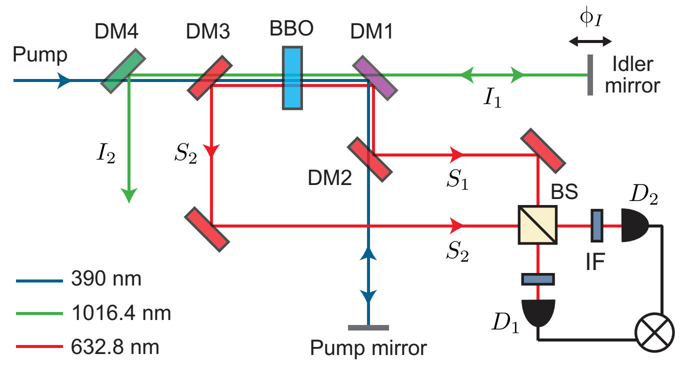

Fig. 2. Experimental setup. Experimental setup corresponding to the schematic shown in Fig. 1B. The idler modes I_1 and I_2 are overlapped by reflecting I_1 with the idler mirror. DM, dichroic mirror; IF, interference filter; BS, beam splitter.

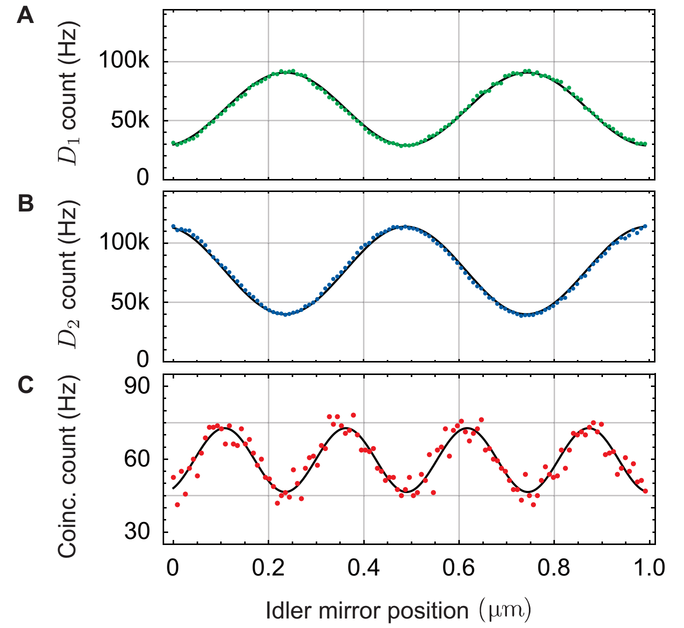

Fig. 3. Experimental results. Quantum interference at D_1 (**A**) and D_2 (**B**) corresponds to the usual induced coherence without induced emission. (**C**) Two-photon induced coherence without induced emission observed in coincidence counts. The signal photon exhibits $2\phi_I$ phase modulation, the hallmark effect for quantum-enhanced sensing in quantum metrology. The solid lines represent the sinusoidal fits to the data points.

data correspond to the usual induced coherence without induced emission. Note that, because ϕ_I is added to the undetected 1016.4-nm idler photon, detectors D_1 and D_2 registering the 632.8-nm signal photons exhibit the modulation period of 1016.4 nm. The observed quantum interference visibilities are 51.7% and 47.8% for Fig. 3 (A and B, respectively).

The experimental data for two-photon induced coherence without induced emission are shown in Fig. 3C. As mentioned earlier, the coincidence event between detectors D_1 and D_2 behind BS in Fig. 1B picks up only the two-photon induced coherence terms in Eq. 1 as the single-photon term is canceled out due to the Shih-Alley/Hong-Ou-Mandel interference at the BS. In this case, the signal photons exhibit $2\phi_I$ phase modulation compared to the case of single photons, evidenced by the interferometric fringe period of 508.2 nm. The experimental data clearly demonstrate quantum-enhanced sensitivity of two-photon induced coherence without induced emission. The two-photon interference visibility is calculated to be 22%. Somewhat lower two-photon interference visibility is attributed to a slight mode mismatch between the idler modes I_1 and I_2, stemming from a number of factors, including spatial mode mismatch, differences in beam divergence, and channel loss due to nonideal transmittance/reflectance of the mirrors, among others. Note that in our experimental configuration, coincidence detection between D_1 and D_2 requires the generation of two photon pairs, as a single pair cannot lead to simultaneous clicks at two spatially separated detectors in the signal path. A product of first-order effects cannot result in a nonzero second-order coincidence, because the detections are mutually exclusive in our configuration. That is, when detector D_1 registers a click, detector D_2 necessarily has no click, and vice versa. See the Supplementary Materials for details.

The effect of temporal mode mismatch is also explored, and the data are shown in Fig. 4A (*49–53*). The idler mirror in Fig. 2 is set at five different positions, namely, −35, −15, 0, 15, and 35 μm, and the maximum and minimum coincidence counts of the two-photon interference near these positions are recorded. The results show the envelope of the two-photon interference with respect to the balanced position of the idler mirror because the visibility of the two-photon interference decreases as the idler mirror is positioned away from the balanced position. In other words, two-photon induced coherence is weakened due to the temporal mismatch, which introduces distinguishability. The result of the full multimode numerical simulation is plotted in Fig. 4B and is in good agreement with the experimental data in Fig. 4A. The inset in Fig. 4B shows the two-photon interference fringe near the center position of the idler mirror, confirming $2\phi_I$ phase modulation or the period of 508.2 nm. See Materials and Methods for details of the calculation.

DISCUSSION

To ensure that induced emission is not present, we place a detector in S_2 mode before BS and compare the single-photon count rates before and after unblocking the undetected photon mode I_1. If induced emission is present when I_1 mode is unblocked, a detector placed in S_2 mode will show an increased count rate compared to the case of I_1 mode blocked. Initially I_1 mode is blocked and the single count rate is continuously measured. At 200 s, I_1 mode is unblocked. The experimental data are shown in Fig. 5. There is no observable increase in the single photon count rate when I_1 mode is unblocked, which confirms the absence of induced emission in our experiment. We have also compared the rates of the two-photon event at S_2, before BS with two single-photon detectors and a beam splitter, before

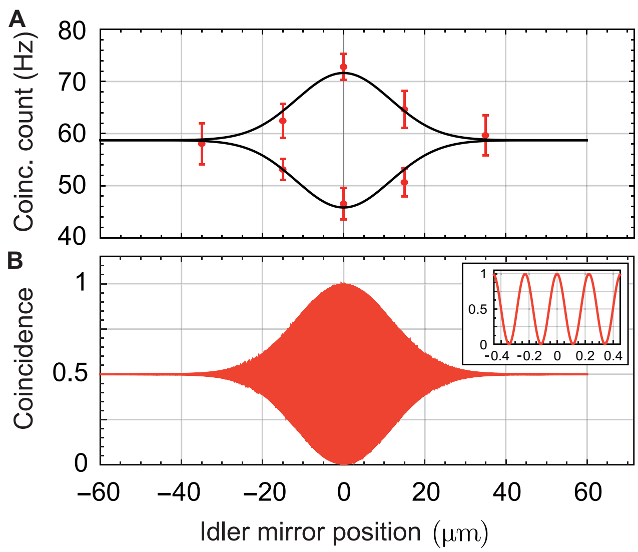

Fig. 4. Effects of temporal mode mismatch. (**A**) Maximum and minimum coincidence counts are recorded for a few different idler mirror positions. The error bars represent 1 SD. The solid lines represent the Gaussian fits to the data points, showing the envelope of the two-photon induced coherence. (**B**) Numerical simulation of two-photon interference fringes, showing the full envelope of the two-photon induced coherence. The inset shows the interference fringe at the center, exhibiting a period of 508.2 nm.

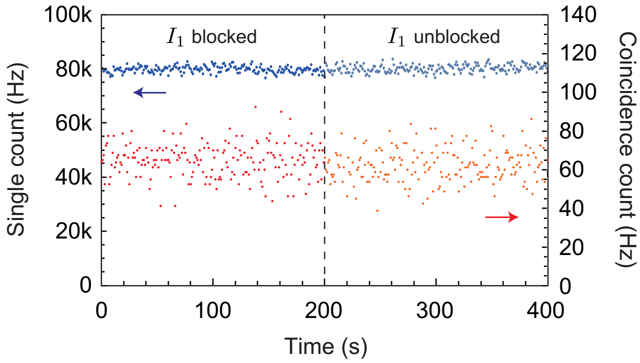

Fig. 5. Absence of induced two-photon emission. Single count and two-photon coincidence count rates in S_2 mode before and after unblocking the undetected photon mode I_1. The data confirm the absence of induced two-photon emission in our experiment.

and after unblocking the undetected photon mode I_1. The coincidence rate also confirms the absence of induced emission in our experiment. See the Supplementary Materials for details.

In conclusion, we have proposed, analyzed, and experimentally demonstrated two-photon induced coherence without induced emission. Although induced coherence without induced emission lies at the heart of recent breakthroughs in quantum optical metrology using undetected photons, thereby opening possibilities in accessing challenging wavelength regimes in various applications, quantum-enhanced phase sensitivity, the hallmark feature of quantum metrology, has not been demonstrated for quantum metrology with undetected photons. This is because the exploration of induced coherence without induced emission has so far been limited to phenomena involving single photons. In our demonstration of the two-photon induced coherence without induced emission, we clearly show a doubling of the interferometric phase modulation compared to what is observed with single photons. Specifically, a phase change ϕ applied to undetected 1016-nm near-infrared photons leads to 2ϕ modulation in the detection of the 632-nm visible photons, verifying quantum-enhanced phase sensitivity corresponding to a two-photon state for quantum metrology with undetected photons. These findings pave the way for innovative quantum-enhanced metrological applications leveraging multiphoton induced coherence without induced emission.

MATERIALS AND METHODS

Theoretical calculation for the two-photon induced coherence effect

The quantum state of SPDC with two photon pairs is written as

$$|\Psi\rangle = \int d\omega_s d\omega_i d\omega_{s'} d\omega_{i'} f(\omega_s,\omega_i) f(\omega_{s'},\omega_{i'}) \times \Big\{ e^{i\phi(\omega_i)} \hat{a}^\dagger_{S_1}(\omega_s)\hat{a}^\dagger_{S_2}(\omega_{s'})\hat{a}^\dagger_{I_1}(\omega_i)\hat{a}^\dagger_{I_2}(\omega_{i'}) + \frac{1}{2} e^{i[\phi(\omega_i)+\phi(\omega_{i'})]}\hat{a}^\dagger_{S_1}(\omega_s)\hat{a}^\dagger_{S_1}(\omega_{s'})\hat{a}^\dagger_{I_1}(\omega_i)\hat{a}^\dagger_{I_1}(\omega_{i'}) + \frac{1}{2}\hat{a}^\dagger_{S_2}(\omega_s)\hat{a}^\dagger_{S_2}(\omega_{s'})\hat{a}^\dagger_{I_2}(\omega_i)\hat{a}^\dagger_{I_2}(\omega_{i'}) \Big\} |0\rangle \quad (3)$$

where $f(\omega_s, \omega_i)$ is a joint spectral amplitude of photon pair and $\hat{a}^\dagger$ is a creation operator. The first term in Eq. 3 corresponds to the case where one photon pair is generated via the forward SPDC process and the other photon pair is generated via the backward SPDC process. The second and the third terms correspond to the case where the two photon pairs are generated via the forward and backward SPDC process, respectively. After mode matching $\hat{a}^\dagger_{I_1}(\omega) \rightarrow \hat{a}^\dagger_{I_2}(\omega)$, the quantum state becomes

$$|\Psi\rangle = \int d\omega_s d\omega_i d\omega_{s'} d\omega_{i'} f(\omega_s,\omega_i) f(\omega_{s'},\omega_{i'}) \times \Big\{ e^{i\phi(\omega_i)} \hat{a}^\dagger_{S_1}(\omega_s)\hat{a}^\dagger_{S_2}(\omega_{s'}) + \frac{1}{2} e^{i[\phi(\omega_i)+\phi(\omega_{i'})]}\hat{a}^\dagger_{S_1}(\omega_s)\hat{a}^\dagger_{S_1}(\omega_{s'}) + \frac{1}{2}\hat{a}^\dagger_{S_2}(\omega_s)\hat{a}^\dagger_{S_2}(\omega_{s'}) \Big\} \hat{a}^\dagger_{I_2}(\omega_i)\hat{a}^\dagger_{I_2}(\omega_{i'}) |0\rangle \quad (4)$$

After passing through the BS, the creation operators transform accordingly, $\hat{a}^\dagger_{S_1}(\omega) \rightarrow \frac{1}{\sqrt{2}}\left[\hat{a}^\dagger_{S_1}(\omega) + i\hat{a}^\dagger_{S_2}(\omega)\right]$ and $\hat{a}^\dagger_{S_2}(\omega) \rightarrow \frac{1}{\sqrt{2}}\left[i\hat{a}^\dagger_{S_1}(\omega) + \hat{a}^\dagger_{S_2}(\omega)\right]$. With an assumption that the joint spectral amplitude is separable, the quantum state becomes

$$|\Psi\rangle = \int d\omega_s d\omega_i d\omega_{s'} d\omega_{i'} f(\omega_s,\omega_i) f(\omega_{s'},\omega_{i'}) \times \Big(\Big\{ \frac{i}{2} e^{i\phi(\omega_i)} + \frac{1}{4} e^{i[\phi(\omega_i)+\phi(\omega_{i'})]} - \frac{1}{4} \Big\} \hat{a}^\dagger_{S_1}(\omega_s)\hat{a}^\dagger_{S_1}(\omega_{s'}) + \Big\{ \frac{i}{2} e^{i\phi(\omega_i)} - \frac{1}{4} e^{i[\phi(\omega_i)+\phi(\omega_{i'})]} + \frac{1}{4} \Big\} \hat{a}^\dagger_{S_2}(\omega_s)\hat{a}^\dagger_{S_2}(\omega_{s'}) + \Big\{ \frac{i}{2} e^{i[\phi(\omega_i)+\phi(\omega_{i'})]} + \frac{i}{2} \Big\} \hat{a}^\dagger_{S_1}(\omega_s)\hat{a}^\dagger_{S_2}(\omega_{s'}) \Big) \times \hat{a}^\dagger_{I_2}(\omega_i)\hat{a}^\dagger_{I_2}(\omega_{i'}) |0\rangle \quad (5)$$

The coincidence detection probability is given as $P = \mathrm{Tr}\left[\left(\hat{D}_{S_1} \otimes \hat{D}_{S_2}\right)\rho_s\right]$, where $\rho_s = \mathrm{Tr}_{I_2}[\,|\Psi\rangle\langle\Psi|\,]$ is the quantum state in front of the detectors after tracing out the idler mode and $\hat{D}_{S_i} = \int d\omega \hat{a}^\dagger_{S_i}(\omega)|0\rangle\langle 0|\hat{a}_{S_i}(\omega)$ is a projection operator. Last, the coincidence detection probability is calculated to be

$$P = \int d\omega_s d\omega_i d\omega_{s'} d\omega_{i'} |f(\omega_s,\omega_i)|^2 |f(\omega_{s'},\omega_{i'})|^2 \{2 + 2\cos[\phi(\omega_i) + \phi(\omega_{i'})]\} \quad (6)$$

For evaluating the above result numerically, all parameters are set to the experimental conditions, and the phase terms $\phi(\omega)$ are given as $2\omega x / c$, where x is a displacement of the idler mirror shown in Fig. 2. Figure 4B shows the numerical simulation result of Eq. 6 as a function of displacement x of the idler mirror.

Supplementary Materials

This PDF file includes:
Supplementary Text
Figs. S1 to S7

REFERENCES AND NOTES

1. C. L. Tang, H. Statz, Phase-locking of laser oscillators by injected signal. *J. Appl. Phys.* **38**, 323–324 (1967).
2. H. L. Stover, W. H. Steier, Locking of laser oscillators by light injection. *Appl. Phys. Lett.* **8**, 91–93 (1966).
3. A. V. Sergienko, Y. H. Shih, M. H. Rubin, Study of induced temporal coherence in optical parametric down conversion. *J. Mod. Opt.* **40**, 1425–1429 (1993).
4. X. Y. Zou, L. J. Wang, L. Mandel, Induced coherence and indistinguishability in optical interference. *Phys. Rev. Lett.* **67**, 318–321 (1991).
5. L. J. Wang, X. Y. Zou, L. Mandel, Induced coherence without induced emission. *Phys. Rev. A* **44**, 4614–4622 (1991).
6. P. G. Kwiat, A. M. Steinberg, R. Y. Chiao, Three proposed "quantum erasers". *Phys. Rev. A* **49**, 61–68 (1994).
7. Y.-H. Kim, R. Yu, S. P. Kulik, Y. Shih, M. O. Scully, Delayed "choice" quantum eraser. *Phys. Rev. Lett.* **84**, 1–5 (2000).

8. Y.-H. Kim, M. V. Chekhova, S. P. Kulik, Y. Shih, M. H. Rubin, First-order interference of nonclassical light emitted spontaneously at different times. *Phys. Rev. A* **61**, 051803 (2000).
9. Y.-H. Kim, W. P. Grice, Quantum interference with distinguishable photons through indistinguishable pathways. *J. Opt. Soc. Am. B* **22**, 493–498 (2005).
10. T. P. Grayson, J. R. Torgerson, G. A. Barbosa, Observation of a nonlocal Pancharatnam phase shift in the process of induced coherence without induced emission. *Phys. Rev. A* **49**, 626–628 (1994).
11. T. P. Grayson, G. A. Barbosa, Spatial properties of spontaneous parametric down-conversion and their effect on induced coherence without induced emission. *Phys. Rev. A* **49**, 2948–2961 (1994).
12. M. Lahiri, A. Hochrainer, R. Lapkiewicz, G. B. Lemos, A. Zeilinger, Nonclassicality of induced coherence without induced emission. *Phys. Rev. A* **100**, 053839 (2019).
13. C. K. Hong, Z. Y. Ou, L. Mandel, Measurement of subpicosecond time intervals between two photons by interference. *Phys. Rev. Lett.* **59**, 2044–2046 (1987).
14. Y.-H. Kim, M. V. Chekhova, S. P. Kulik, Y. Shih, Quantum interference by two temporally distinguishable pulses. *Phys. Rev. A* **60**, R37–R40 (1999).
15. Y.-H. Kim, V. Berardi, M. V. Chekhova, A. Garuccio, Y. Shih, Temporal indistinguishability and quantum interference. *Phys. Rev. A* **62**, 043820 (2000).
16. A. V. Burlakov, M. V. Chekhova, D. N. Klyshko, S. P. Kulik, A. N. Penin, Y. H. Shih, D. V. Strekalov, Interference effects in spontaneous two-photon parametric scattering from two macroscopic regions. *Phys. Rev. A* **56**, 3214–3225 (1997).
17. D. Y. Korystov, S. P. Kulik, A. N. Penin, Rozhdestvenski hooks in two-photon parametric light scattering. *Theor. Phys. Lett.* **73**, 214–218 (2001).
18. S. P. Kulik, G. A. Maslennikov, S. P. Merkulova, A. N. Penin, L. K. Radchenko, V. N. Krasheninnikov, Two-photon interference in the presence of absorption. *J. Exp. Theor. Phys.* **98**, 31–38 (2004).
19. M. V. Chekhova, Z. Y. Ou, Nonlinear interferometers in quantum optics. *Adv. Opt. Photon.* **8**, 104–155 (2016).
20. G. B. Lemos, V. Borish, G. D. Cole, S. Ramelow, R. Lapkiewicz, A. Zeilinger, Quantum imaging with undetected photons. *Nature* **512**, 409–412 (2014).
21. M. Lahiri, R. Lapkiewicz, G. B. Lemos, A. Zeilinger, Theory of quantum imaging with undetected photons. *Phys. Rev. A* **92**, 013832 (2015).
22. I. Kviatkovsky, H. M. Chrzanowski, E. G. Avery, H. Bartolomaeus, S. Ramelow, Microscopy with undetected photons in the mid-infrared. *Sci. Adv.* **6**, eabd0264 (2020).
23. E. A. Santos, T. Pertsch, F. Setzpfandt, S. Saravi, Subdiffraction quantum imaging with undetected photons. *Phys. Rev. Lett.* **128**, 173601 (2022).
24. A. Vega, E. A. Santos, J. Fuenzalida, M. Gilaberte Basset, T. Pertsch, M. Gräfe, S. Saravi, F. Setzpfandt, Fundamental resolution limit of quantum imaging with undetected photons. *Phys. Rev. Res.* **4**, 033252 (2022).
25. J. Fuenzalida, M. Gilaberte Basset, S. Töpfer, J. P. Torres, M. Gräfe, Experimental quantum imaging distillation with undetected light. *Sci. Adv.* **9**, eadg9573 (2023).
26. T. B. Pittman, Y. H. Shih, D. V. Strekalov, A. V. Sergienko, Optical imaging by means of two-photon quantum entanglement. *Phys. Rev. A* **52**, R3429(R) (1995).
27. D. V. Strekalov, A. V. Sergienko, D. N. Klyshko, Y. H. Shih, Observation of two-photon "Ghost" interference and diffraction. *Phys. Rev. Lett.* **74**, 3600–3603 (1995).
28. J.-E. Oh, Y.-W. Cho, G. Scarcelli, Y.-H. Kim, Sub-Rayleigh imaging via speckle illumination. *Opt. Lett.* **38**, 682–684 (2013).
29. Y. Yang, H. Liang, X. Xu, L. Zhang, S. Zhu, X. Ma, Interaction-free, single-pixel quantum imaging with undetected photons. *npj Quantum Inf.* **9**, 2 (2023).
30. D. A. Kalashnikov, A. V. Paterova, S. P. Kulik, L. A. Krivitsky, Infrared spectroscopy with visible light. *Nat. Photon.* **10**, 98–101 (2016).
31. A. Paterova, S. Lung, D. A. Kalashnikov, L. A. Krivitsky, Nonlinear infrared spectroscopy free from spectral selection. *Sci. Rep.* **7**, 42608 (2017).
32. A. V. Paterova, H. Yang, C. An, D. A. Kalashnikov, L. A. Krivitsky, Measurement of infrared optical constants with visible photons. *New J. Phys.* **20**, 043015 (2018).
33. A. V. Paterova, S. M. Maniam, H. Yang, G. Grenci, L. A. Krivitsky, Hyperspectral infrared microscopy with visible light. *Sci. Adv.* **6**, eabd0460 (2020).
34. A. V. Paterova, H. Yang, C. An, D. A. Kalashnikov, L. A. Krivitsky, Tunable optical coherence tomography in the infrared range using visible photons. *Quantum Sci. Technol.* **3**, 025008 (2018).
35. A. Vallés, G. Jiménez, L. J. Salazar-Serrano, J. P. Torres, Optical sectioning in induced coherence tomography with frequency-entangled photons. *Phys. Rev. A* **97**, 023824 (2018).
36. A. V. Paterova, H. Yang, C. An, D. Kalashnikov, L. Krivitsky, Polarization effects in nonlinear interference of down-converted photons. *Opt. Express* **27**, 2589–2603 (2019).
37. B. Yurke, M. Potasek, Obtainment of thermal noise from a pure quantum state. *Phys. Rev. A* **36**, 3464–3466 (1987).
38. D. V. Strekalov, Y.-H. Kim, Y. Shih, Experimental study of a subsystem in an entangled two-photon state. *Phys. Rev. A* **60**, 2685–2688 (1999).
39. I. Afek, O. Ambar, Y. Silberberg, High-NOON states by mixing quantum and classical light. *Science* **328**, 879–881 (2010).
40. Y.-S. Kim, O. Kwon, S. M. Lee, J.-C. Lee, H. Kim, S.-K. Choi, H. S. Park, Y.-H. Kim, Observation of Young's double-slit interference with the three-photon N00N state. *Opt. Express* **19**, 24957–24966 (2011).
41. Y.-S. Ra, M. C. Tichy, H.-T. Lim, O. Kwon, F. Mintert, A. Buchleitner, Y.-H. Kim, Observation of detection-dependent multi-photon coherence times. *Nat. Commun.* **4**, 2451 (2013).
42. S. Pang, J. Dressel, T. A. Brun, Entanglement-assisted weak value amplification. *Phys. Rev. Lett.* **113**, 030401 (2014).
43. S. Hong, J. Ur Rehman, Y.-S. Kim, Y.-W. Cho, S.-W. Lee, H. Jung, S. Moon, S.-W. Han, H.-T. Lim, Quantum enhanced multiple-phase estimation with multi-mode N00N states. *Nat. commun.* **12**, 5211 (2021).
44. Y. Kim, S.-Y. Yoo, Y.-H. Kim, Heisenberg-limited metrology via weak-value amplification without using entangled resources. *Phys. Rev. Lett.* **128**, 040503 (2022).
45. Y.-H. Kim, W. P. Grice, Measurement of the spectral properties of the two-photon state generated via type II spontaneous parametric downconversion. *Opt. Lett.* **30**, 908–910 (2005).
46. P. J. Mosley, J. S. Lundeen, B. J. Smith, P. Wasylczyk, A. B. U'Ren, C. Silberhorn, I. A. Walmsley, Heralded generation of ultrafast single photons in pure quantum states. *Phys. Rev. Lett.* **100**, 133601 (2008).
47. F. Kaneda, K. Garay-Palmett, A. B. U'Ren, P. G. Kwiat, Heralded single-photon source utilizing highly nondegenerate, spectrally factorable spontaneous parametric downconversion. *Opt. Express* **24**, 10733–10747 (2016).
48. X.-L. Wang, L.-K. Chen, W. Li, H.-L. Huang, C. Liu, C. Chen, Y.-H. Luo, Z.-E. Su, D. Wu, Z.-D. Li, H. Lu, Y. Hu, X. Jiang, C.-Z. Peng, L. Li, N.-L. Liu, Y.-A. Chen, C.-Y. Lu, J.-W. Pan, Experimental ten-photon entanglement. *Phys. Rev. Lett.* **117**, 210502 (2016).
49. Y.-H. Kim, Measurement of one-photon and two-photon wave packets in spontaneous parametric downconversion. *J. Opt. Soc. Am. B* **20**, 1959–1966 (2003).
50. O. Kwon, Y.-S. Ra, Y.-H. Kim, Coherence properties of spontaneous parametric down-conversion pumped by a multi-mode cw diode laser. *Opt. Express* **17**, 13059–13069 (2009).
51. Y. S. Ihn, Y. Kim, V. Tamma, Y.-H. Kim, Second-order temporal interference with thermal light: Interference beyond the coherence time. *Phys. Rev. Lett.* **119**, 263603 (2017).
52. G.-H. Lee, D.-G. Im, Y. Kim, U.-S. Kim, Y.-H. Kim, Observation of second-order interference beyond the coherence time with true thermal photons. *Opt. Lett.* **45**, 6748–6751 (2020).
53. C.-H. Lee, Y. Kim, D.-G. Im, U.-S. Kim, V. Tamma, Y.-H. Kim, Coherent two-photon LIDAR with incoherent light. *Phys. Rev. Lett.* **131**, 223602 (2023).

Acknowledgments

Funding: Y.-H.K. acknowledges the National Research Foundation of Korea (RS-2023-00208500 and RS-2024-00442762) and the Ministry of Science and ICT of Korea under the Information Technology Research Center support program (IITP-2025-RS-2022-00164799). **Author contributions:** Conceptualization: D.-G.I., C.-H.L., S.-Y.Y., and Y.-H.K. Methodology: D.-G.I. and Y.-H.K. Investigation: D.-G.I., C.-H.L., S.-Y.Y., and Y.-H.K. Visualization: D.-G.I. and Y.-H.K. Formal analysis: D.-G.I., C.-H.L., J.S., and Y.-H.K. Supervision: D.-G.I. and Y.-H.K. Writing—original draft: D.-G.I. and Y.-H.K. Writing—review and editing: D.-G.I., C.-H.L., S.-Y.Y., J.S., and Y.-H.K. **Competing interests:** The authors declare that they have no competing interests. **Data and materials availability:** All data needed to evaluate the conclusions in the paper are present in the paper and/or the Supplementary Materials.

Submitted 4 March 2025
Accepted 23 October 2025
Published 21 November 2025
10.1126/sciadv.adx2038